Communications on Applied Nonlinear Analysis
ISSN: 1074-133X
Vol 32 No. 8s (2025)

Pruned DFT based FBMC employing PPN with Low Latency Low PAPR

Prathyusha V [a], E.Sreenivasa Rao [b]

[a] Research scholar, Department of ECE, University College of Engg, Osmania University, Hyderabad-500007, India

[b]Professor, Department of ECE, Vasavi College of Engg., Hyderabad,India.

Email id: prathyusha.velijala@gmail.com, e.sreenivasarao@staff.vce.ac.in

Article History:

Received: *27-10-2024*

Revised: *16-11-2024*

Accepted: *18-12-2024*

Abstract:

Future wireless systems must accommodate a diverse range of practical applications within a particular frequency spectrum.This is a hurdle for earlier CP-OFDM owing to insufficient out-of-band emissions. Because of its considerable spectrum features, FBMC is an efficient alternative to OFDM for future wireless system use cases that do not need a large number of subcarriers. Although FBMC offers several benefits, it requires special supervision owing to the inherent fictional interference.In most real-world scenarios, one-tap equalizers are enough for FBMC, provided the subcarrier frequency aligns with the channel. By dispersing symbols that represent data throughout time or frequency, accurate orthogonality can potentially be restored in FBMC-OQAM, facilitating the immediate implementation of all OFDM techniques. This work's important addition is that the PrunedDFT spread FBMC outperforms SCFDMA in almost every dimension. It demonstrates greater resilience in doubly-selective channels, eliminates cyclic prefixes, and significantly reduces out-of-band emissions. Utilizing trimmed DFT spread FBMC has become preferable for throughput over regular FBMC-OQAM whenever the channel remains nearly uniform over the entire transmission bandwidth.

Keywords: FBMC, OFDM, OQAM.

1. Introduction

"Filter Bank Multi-Carrier," is a great modulation method for future wireless systems because it makes a lot less Out-Of-Band (OOB) emissions than Orthogonal Frequency Division Multiplexing (OFDM) [1]. It is also sometimes just called "FBMC." This makes asynchronous transmissions more efficient and makes it easier to find the best time-frequency allocation for different uses [2]. Moreover, FBMC generally is not required to have a cyclic prefix (CP), hence enhancing throughput. In order to meet the Balian-Low theorem [3], FBMC replaces the strict orthogonality requirement with a less strict real orthogonality requirement. This causes intrinsic interference, which mostly affects the imaginary part, which makes channel estimation [4] and multiple-input multiple-output (MIMO) [5, 6] more difficult. Researchers have proposed various approaches to tackle these difficulties [2], [7], [8].For example, complex orthogonality can be brought back to FBMC by spreading symbols out over time. This makes it possible to use almost all OFDM detection techniques directly [2]. The technique is effective if the channel remains relatively level over the spreading duration. As suggested in [6], we can base the spreading on the discrete Fourier transform (DFT) dispersion over a period of time. Despite the channel's relative flatness, our study in [9], [10] demonstrates that Walsh-Hadamard spread [5], [11] outperforms DFT spreading by more efficiently restoring complex orthogonality inside a single block and necessitating less computational resources. Nonetheless, DFT spreading has become advantageous since it organizes the transmitted signal temporally and reduces the Peak-to-Average Power Ratio (PAPR). In addition to interference that comes with the territory, nonlinearities such as limited DAC resolution and nonlinear power amplifiers make real-world systems very difficult to use because they make it harder for Filter Bank Multicarrier (FBMC) to keep the spectrum tightly contained [2, 12]. Consequently, FBMC remains only effective when functioning within a suitably linear domain. Regarding multi-carrier structures, achieving this is challenging because of the inadequate Peak-to-Average Power Ratio (PAPR). Researchers have proposed various approaches [13,14], to mitigate the PAPR in OFDM. As demonstrated in [15]–[17], we can use the aforementioned approaches for FBMC. Nonetheless, all those strategies need significant computing complexity and auxiliary information. These disadvantages demonstrate why these functions are rarely used in actual systems. Single Carrier Frequency-Division Multiple Access (SC-FDMA), which is essentially a DFT precoded OFDM system, is used for the uplink in Long Term Evolution (LTE). Fifth Generation (5G) wireless communication networks will also incorporate this technology as an alternative in the uplink, alongside CP-OFDM [19]. Unfortunately, just combining FBMC with a DFT, similar to SC-FDMA, results in inadequate efficiency for FBMC [20]–[22]. The researchers in [20] recommend use a filter bank in precoding to improve performance, instead than utilizing a DFT. Although this technology reduces PAPR, it remains inferior to SC-FDMA and has additional challenges such as increased expenses and more complex computations.

In [22], researchers showed that a basic DFT spread FBMC method is different from traditional FBMC in that it has an extra phase term that changes how well it works for PAPR. Nonetheless, even with the inclusion of an ideal phase period, the PAPR remains inferior to that of SC-FDMA. The authors in [22] offer a selection strategy.A number of researchers have suggested an alternate approach; nonetheless, it is characterized by significant complexity, suboptimal latency, and increased side lobes. To tackle these issues, we suggest an innovative modulation approach that employs a diminished DFT combined with a single-tap equaliser. This approach facilitates the restoration of intricate orthogonality in FBMC.

The proposed model is analysed regarding PAPR, BER, Throughput. The remainder of this article is organized as follows: Section 2 describes the multi carrier system model. Section 3 explains the proposed pruned DFT dependent FBMC employing PPN , while Section 4 explains the simulation results and corresponding performance analysis. Finally, section 5 explains the conclusion.

2. Multi Carrier System model

A multicarrier system usually links a symbol to the l^{th} subcarrier and the m^{th} position. This is shown as $x_{l,m}$, and it can be changed using either PAM or QAM. The transmitter sustains the essential pulse starting at $g_{l,m}$ and delivers the transmitted signal.

$$s(t) = \sum_{m=1}^{M} \sum_{l=1}^{L} g_{l,m}(t) x_{l,m} \tag{1}$$

Additionally, the transmitted fundamental pulse has been described.

$$g_{l,m}(t) = p(t - mT) e^{j2\pi lF(t-mT)} e^{j\pi/2(l+m)} \tag{2}$$

Wherein

T is referred to be Time space,

F is referred to be Frequency space

The fundamental pulse $g_{l,m}$ represents the prototyping filter $P_T(t)$, and it represents a time and frequency-shifted variant for distinct l & m values. We apply the received signal r(t) to the receiver's basic pulse $q_{l,m,}$ and decode the symbols accordingly.

$$y_{l,m}(t) = \langle r(t), q_{l,m}(t) \rangle = \int_{-\alpha}^{\alpha} r(t) q^{*}_{l,m}(t) dt \tag{3}$$

The receiver prototyping filter $P_R(t)$ defines $q_{l,m}(t)$ to be

$$q_{l,m}(t) = P_{RX}(t - mT) e^{j2\pi lF(t-mT)} e^{j\theta_{l,m} t} \tag{4}$$

The transmitter and receiver have synchronized their basic pulses to achieve the optimal signal-to-noise ratio (SNR) within an AWGN channel. Specifically, $q_{l,m(t)} = g_{l,m(t)}$, and the transmitter and receiver filters must correspond so that $P_T(t) = P_R(t)$. Furthermore, PT(t) cannot be identical to $P_R(t)$ whenever the channel is persistently doubly selective. Therefore, we have defined the approach's ambiguous functionality as follows:

$$A(\tau, \upsilon) = \int_{-\alpha}^{\alpha} P_{TX}(t - \tau/2) P^{*}_{RX}(t + \tau/2) e^{j2\Pi \upsilon t} dt \tag{5}$$

Wherein

τ - time offset

v - frequency offset.

The signal transmission matrix may be described as

$$S = \sum_{m=1}^{M} G_m x_m = Gx \tag{6}$$

Where $S \in C^{N\times 1}$,

The transmitted symbols using time index m would have been labelled by

$$x_m = [x_{1,m}, x_{2,m} \ldots x_{l,m}]^T \in C^{LX1} \tag{7}$$

The Matrix approach, known as G, simplifies mathematical calculations by organizing all fundamental pulses within the transmitter into a matrix.

$$y = R^H (Hs + n) = R^H (HGx + n) = R^H HGx + G^H n \tag{8}$$

$$\approx diag\{h\} R^H Gx + R^H n \tag{9}$$

Wherein, H(t) is represented as time based channel matrix

Because we utilize a matching filtering receiver, the prototype filter becomes equivalent to the transmitter, so $R^H = G^H$.

h – 1-tap channel satisfying the symmetry of OQAM.

3. Pruned DFT dependent FBMC employing PPN

This section presents a technique that surpasses trimmed DFT and offers a comparison study with pruned DFT . The truncated DFT framework has been used using an adaptation of the innovative block associated with the Poly-phase network (PPN). A similar block additionally exists at the receiving end. The subsequent blocks operate in a manner that is comparable to the idea presented in the previous section. All characteristics are produced and modelled via Matlab. This simulation results, together with all design parameters, have been included.

3.1 Representation of the proposed architecture

The suggested method for pDFT distributed FBMC using a polyphasing network can be observed in Fig. 1.

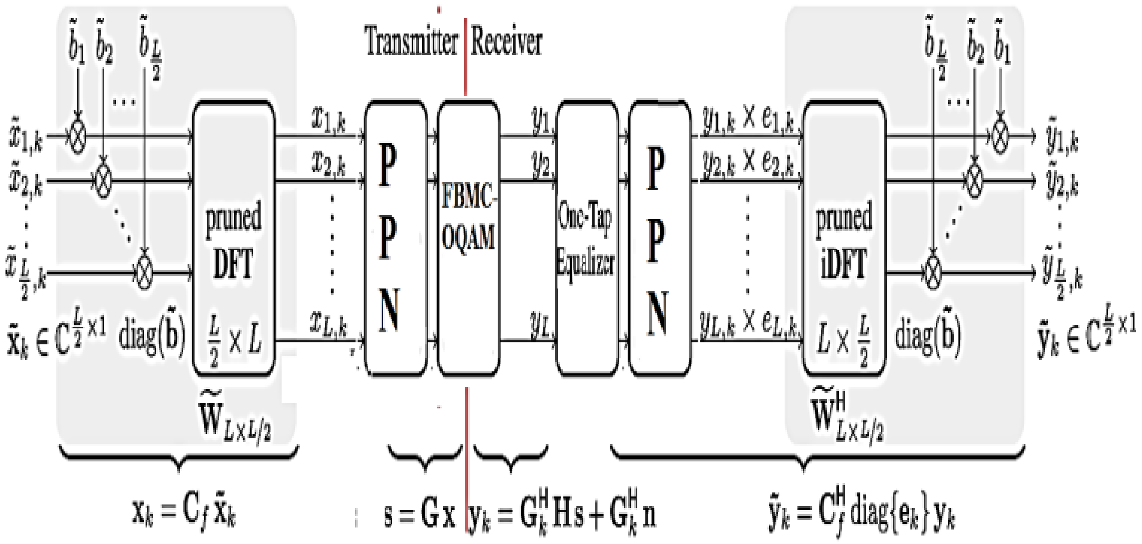

Fig. 1. Representation of of pDFT FBMC using PPN

The essential elements of the transmitter system include: 1) Pruned Discrete Fourier Transform / Inverse Discrete Fourier Transform

2) Transform the PPN transmitter as well as receiver into FBMC-OQAM with a one-tap equalization. A concise summary of every element has been given here.

Pruned DFT/IDFT

Fig.2 illustrates the distinctions in the foundational pulse of OFDM along with its conversion into additional multicarrier schemes. Figure 2 demonstrates that the principles of OFDM consist of frequency-shifted rectangle pulses. Whenever OFDM is precoded, it emulates a DFT single-carrier structure, which includes SC-FDMA. Utilizing decreased DFT for precoded OFDM results in trimmed DFT OFDM. Filtering p-DFT OFDM using a prototyping filter produces unscaled p-DFT FBMC, that is then multiplied by a value to get p-DFT FBMC. The receiver utilizes the pruned IDFT as the inverse function of the truncated DFT.

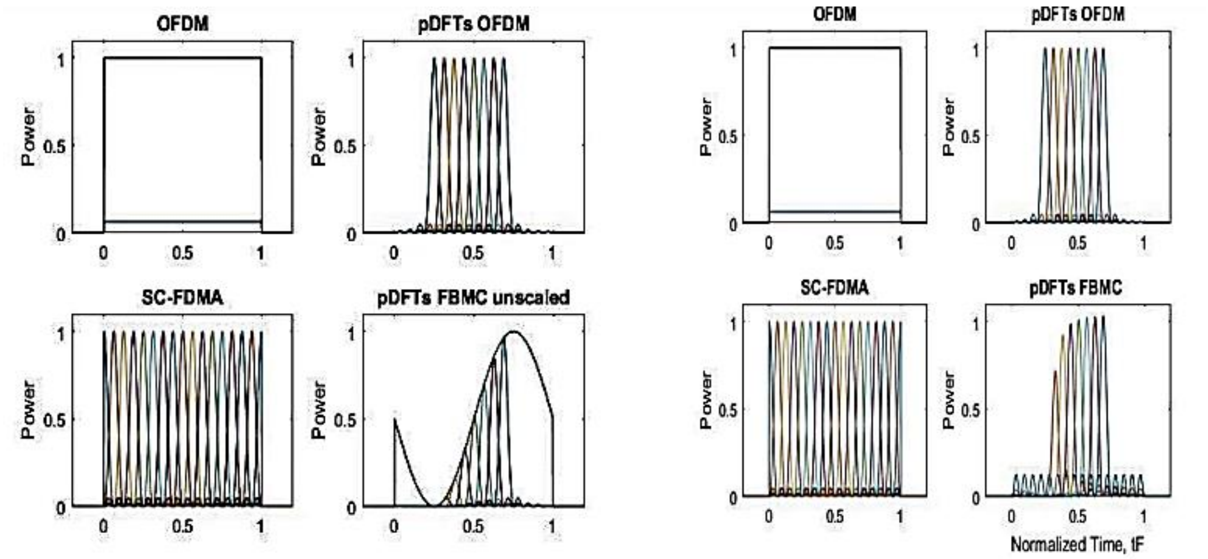

Fig. 2. Representation of the fundamental pulse for different transmission methods

Poly-Phase based Transmission and receiving:

The IFFT information generated by input x l,m has been displayed as IFFT x l,m. The data is subsequently transmitted to the a three-phase system demonstrated in Fig.3. The PPN block provides the basis for overlapping and further filtration. The PPN generates the following output after processing the data:

$$x_{l,m}^{PPN} = \sum_{O=0}^{2O-1} g[On/2+l]\, x_{l,m-o}^{IFFT} \tag{10}$$

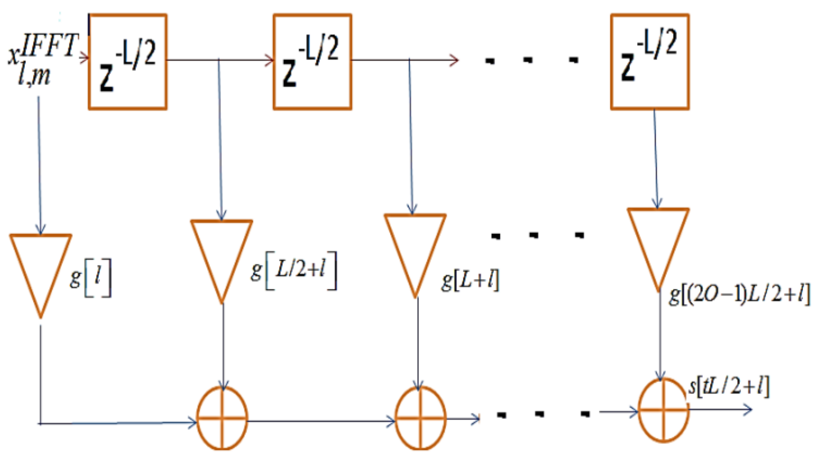

Fig. 3. Depiction of a polyphase network structure

A PPN receiver utilizes a filter that performs downsampling while preserving a matched filter. The data acquired by FBMC, in conjunction with the matching filter, can potentially be articulated as

$$y_{l,m}^{PPN} = \sum_{O=0}^{2O-1} g^{*}[oL/2+l]x_{l,m+O}^{PPN} \tag{11}$$

$$y_m = G^H(Hs+n) = G_l^H\left(HG_l x_l^{PPN} + n\right) = G_l^H HG_l x_l^{PPN} + G_l^H n \tag{12}$$

$$\approx diag\{h\} G_l^H G_l x + G_l^H n \tag{13}$$

The one-tap channel may be designated by h and independently attains genuine orthogonality associated with OQAM.

One-tap equalization:

One-tap equalization can be performed at the receiver on the data that is received symbols, while dispreading has become concurrently executed to provide

$$\tilde{y}_m = C_f^H diag\{e_m\}^{-1} y_m \tag{14}$$

The spreading matrix has been calculated from the assumption of an AWGN channel which does not require equalization. Complex orthogonality would be reinstated to facilitate

$$C_f^H G_m^H G_m C_f \approx I_{L/2} \tag{15}$$

Nevertheless, in diverse contexts, this has little influence on performance. The spreading along with despreading matrix of D_L may be denoted by vector 'a' and articulated as

$$a = diag\{D_L^H G_m^H G_m D_L\} \tag{16}$$

4. Simulation performance evaluation and conclusions

This section describes the simulation process and performance analysis of the presented designs with parameters like transmitted power, throughput.

4.1 Simulation results

Transmitted Power:

Fig. 4 demonstrates that traditional FBMC transmission encompasses a prolonged peak and fall phase resulting from considerable temporal signal overlap. In pDFT-FBMC, as previously mentioned, the temporal overlap gets smaller, leading to a significant decrease in both the length and slope of the downcast phase, since preprogramming by Cf specifies the broadcast signal accordingly.

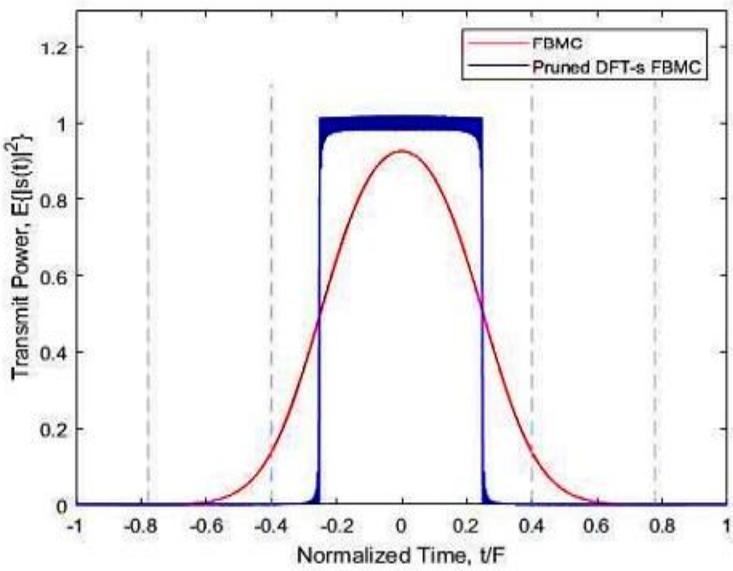

Fig. 4. Transmitting Power of one subcarrier

Power Spectral Density (PSD) :

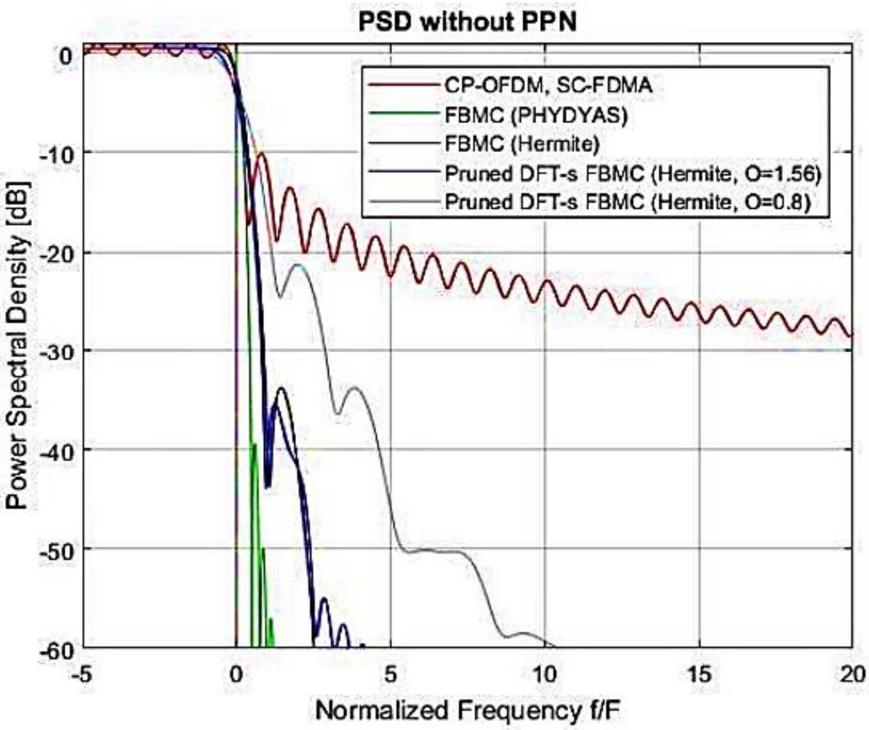

Fig. 5. Analysis of power spectral density excluding PPN

Fig. 5 demonstrates that the trimmed DFT FBMC with PPN surpasses other schemes in the comparative analysis of PSD, resulting in reduced side lobes and thus lowering out-of-band emissions (OOBE). A comparative investigation of PSD indicates that the trimmed DFT FBMC using PPN surpasses other schemes, producing small side lobes and thereby reducing out-of-band emissions (OOBE).

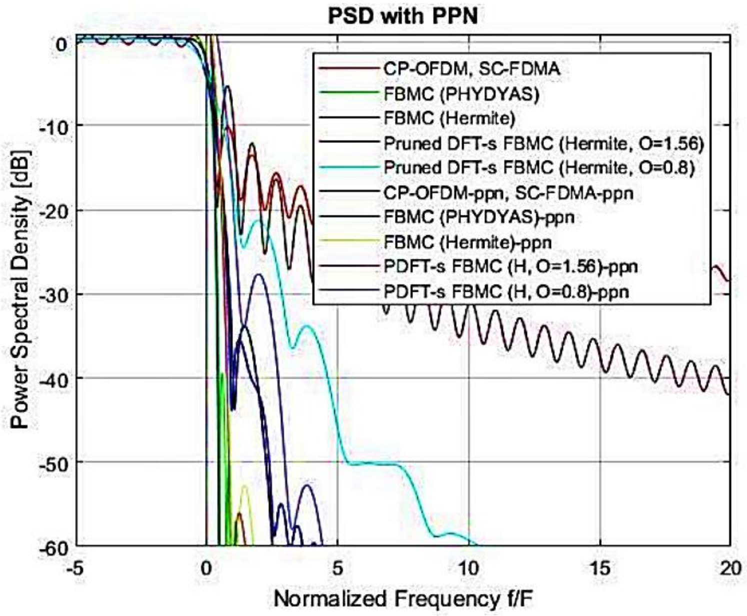

Fig. 6. Analysis of PSD with PPN

Fig. 6 illustrates the PSD of several multicarrier systems using PPN. Consistent with prior findings, we analyzed several systems devoid of PPN and noted that correctly trimmed DFT FBMC employing a Hermite filter with an overlapped coefficient of 0.8 exhibits greater efficiency. All of these structures undergo re-evaluation with PPN, revealing that PPN-based approaches exceed Non-PPN systems. The optimum out-of-band emission (OOBE) performance is attained using the pruned DFT FBMC using PPN, employing a Hermite prototyping filter having an overlapped value equal to 0.8.

Throughput Analysis:

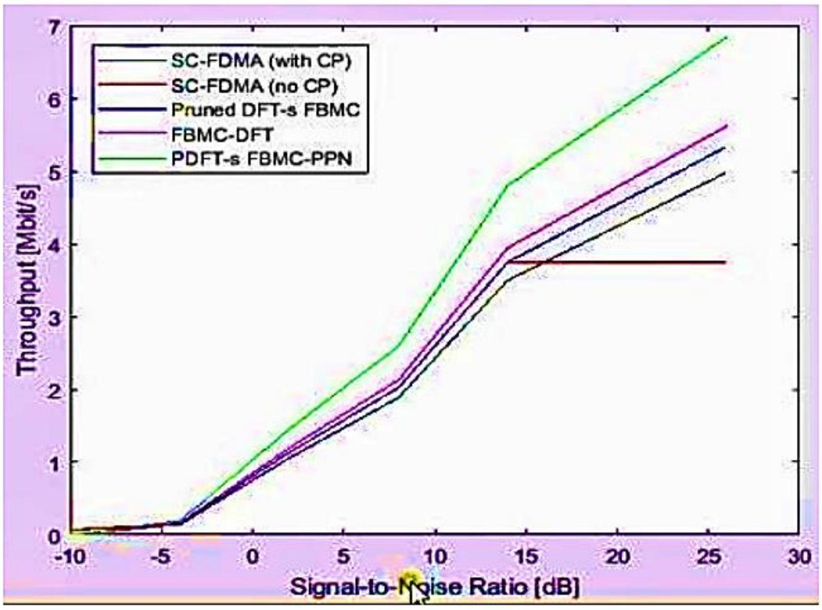

Fig. 7. Throughput Comparison of SC-FDMA and FBMC Schemes

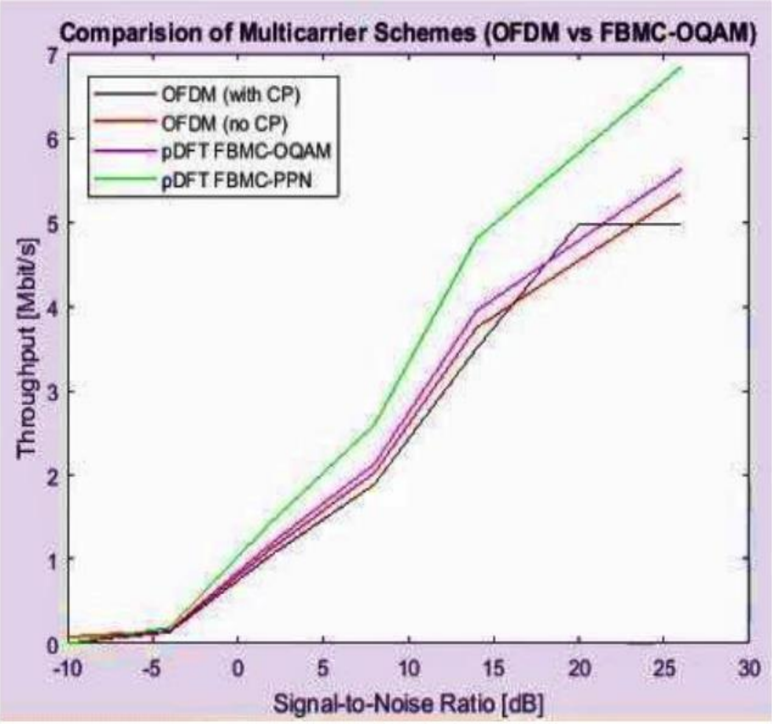

Fig. 8. Throughput comparison of OFDM,FBMC schemes

Figures 7 and 8 show the throughput study of several multicarrier architectures. A distinct assessment of the suggested structure using SC-FDMA as well as OFDM have been presented. Figure 7 demonstrates that our improved DFT FBMC-PPN approach outperforms other methods owing to the elimination of a cyclic prefix. At a SNR around 20 dB, the throughput attained equals 5.5 Mbps for pDFT-FBMC based PPN. Conversely, SCFDMA (lacking a cyclic prefix) achieves 4.5 Mbps, SC-FDMA (containing a cyclic prefix) reaches 4 Mbps, pruned DFT FBMC produces 4.8 Mbps, whereas FBMC-DFT delivers 5 Mbps. Likewise, as demonstrated in Figure 8, the optimized DFT FBMC-PPN method outperforms existing OFDM systems, irrespective of the inclusion of a cyclic prefix containing fundamental characteristics of OFDM & FBMC.

Spectral efficiency:

The dotted lines represent the achievable spectrum efficiency, while the solid lines illustrate the generated throughput, as illustrated in Fig. 9. The attainable rate is established by evaluating the transmission of any information symbol across separate AWGN channels, every characterised by its distinctive SINR, having the capability of every channel being calculated based on BICM capacity. Based on BICM capability, the spectral effectiveness estimate indicates that our approach surpasses trimmed DFT-FBMC in effectiveness. Calculated spectral efficiency demonstrates a 2 dB variation in SNR compared to measured spectral efficiency.

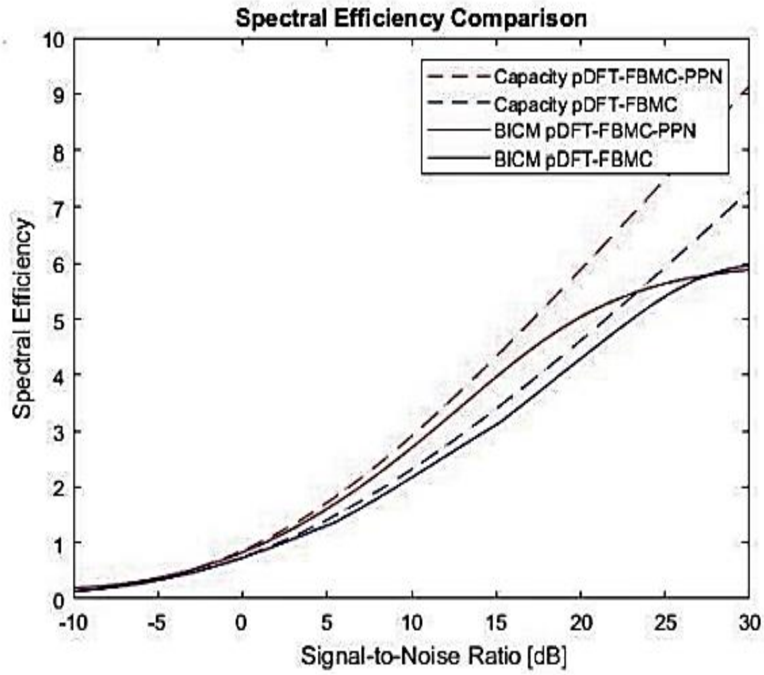

Fig. 9. Spectral efficiency comparison

Comparison of CCDF of PAPR

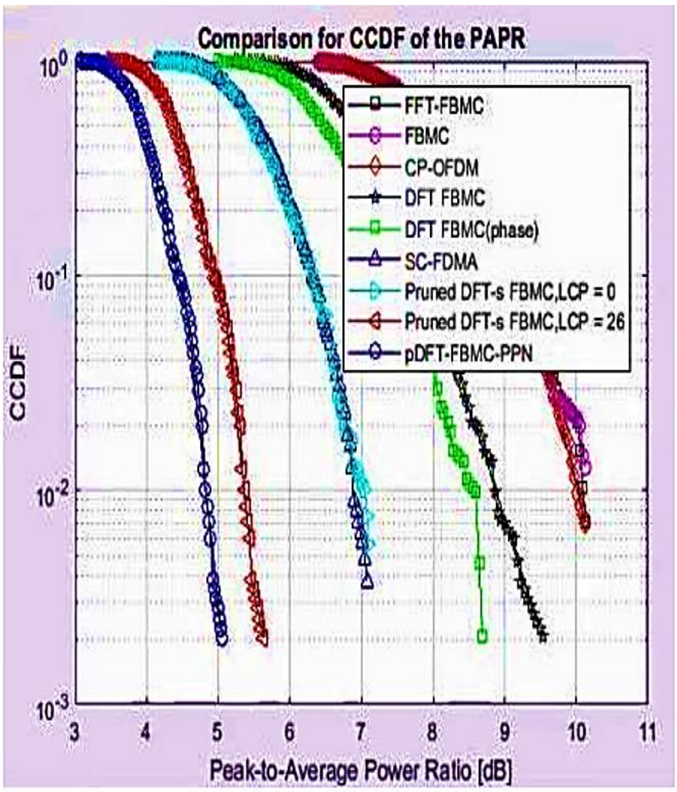

Fig. 10. PAPR Comparison

PAPR constitutes a severe limitation of OFDM, making it unsuitable for most group communication methods. Fig. 10 depicts assessment of PAPR across several systems, along with a comparative study. The research suggests that pDFT-FBMC-PPN exhibits enhanced performance with a decreased PAPR. PAPR may be improved based on the total length of the cyclic prefix (LCP).PDFT-FBMC having a frequency cyclic prefix surpasses pDFT-FBMC without a cyclic prefix. The CCDF may be used to calculate power from a time-domain signal. These graphs indicate the probability of signal intensity surpassing average power.

Bit Error Rate (BER)

We evaluate the error rate associated with received symbols by calculating the Bit Error Rate (BER) about the Signal-to-Noise Ratio (SNR). Fig. 11 demonstrates that the Bit Error Rate (BER) associated with pDFT-FBMC-PPN has been much lower than that of other systems. Our novel transmission methodology employing pDFT FBMC featuring PPN taps for OFDM and SCFDMA across many angles throughout highly selective networks eliminates the need for a cyclic prefix and exhibits satisfactory performance versus out-of-band emissions. Moreover, in the case of a relatively flat network, the proposed method surpasses traditional FBMC by directly addressing MIMO effects.

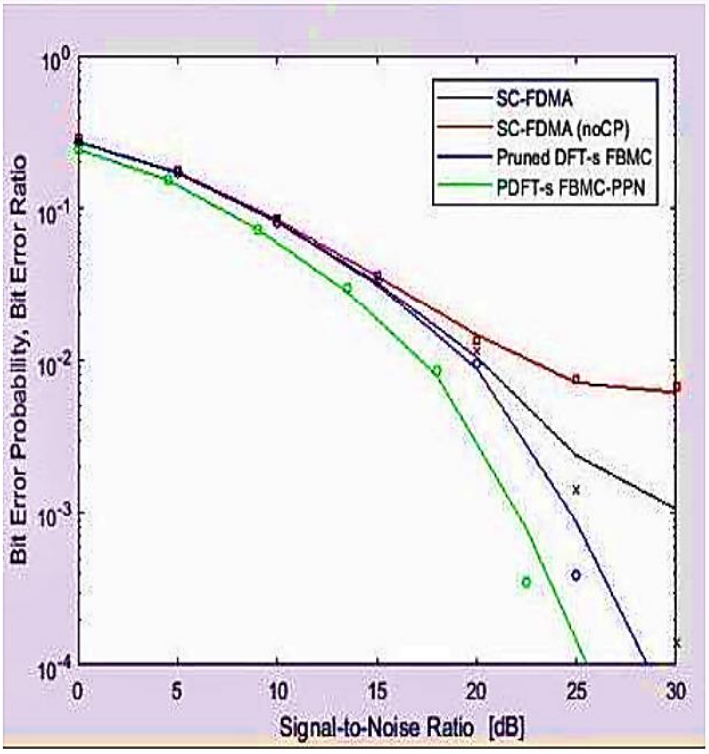

Fig. 11 BER,BEP vs SNR

5 Conclusions

FBMC serves as an effective alternative to OFDM for forthcoming wireless system applications that do not need a substantial number of subcarriers. Despite the advantages of FBMC, it need specialized oversight due to the intrinsic fictitious interference.In most practical situations, one-tap equalizers suffice for FBMC, contingent upon the subcarrier frequency coinciding with the channel.In this work, the pruned DFT spreading FBMC surpasses SCFDMA substantially all respects. It exhibits improved robustness in doubly-selective channels, omits a cyclic prefix, and demonstrates significantly reduced OOB emissions. Within scenarios whenever the channel represents almost flat over the entire transmission spectrum , trimmed DFT spreading FBMC surpasses conventional FBMC-OQAM regarding throughput.

References

[1] B. Farhang-Boroujeny and H. Moradi, "OFDM inspired waveforms for 5G," IEEE Communications Surveys & Tutorials, vol. 18, no. 4, pp. 2474–2492, 2016.

[2] H. G. Feichtinger and T. Strohmer, Gabor analysis and algorithms: Theory and applications. Springer Science & Business Media, 2012.

[3] R. Nissel, S. Schwarz, and M. Rupp, "Filter bank multicarrier modulation schemes for future mobile communications," IEEE Journal on Selected Areas in Communications, vol. 35, no. 8, pp. 1768–1782, 2017.

[4] C. L´el´e, P. Siohan, and R. Legouable, "The Alamouti scheme with CDMA-OFDM/OQAM," EURASIP Journal on Advances in Signal Processing, vol. 2010, Article ID 703513, pp. 1–13, 2010.

[5] D. Katselis, E. Kofidis, A. Rontogiannis, and S. Theodoridis, "Preamblebased channel estimation for CP-OFDM and OFDM/OQAM systems: A comparative study," IEEE Trans. Signal Process., vol. 58, no. 5, pp. 2911–2916, 2010.

[6] R. Zakaria and D. Le Ruyet, "A novel filter-bank multicarrier scheme to mitigate the intrinsic interference: application to MIMO systems," IEEE Transactions on Wireless Communications, vol. 11, no. 3, pp. 1112– 1123, 2012.

[7] M. Caus and A. I. Perez-Neira, "SDMA for filterbank with Tomlinson Harashima precoding," in IEEE International Conference on Communications (ICC), 2013, pp. 4571–4575.

[8] A. I. P´erez Neira, M. Caus, Z. Rostom, D. Le Ruyet, E. Kofidis, M. Haardt, X. Mestre, and Y. Cheng, "MIMO signal processing in offset-QAM based filter bank multicarrier systems," IEEE transactions on signal processing, vol. 64, no. 21, pp. 5733–5762, 2016.

[9] R. Nissel and M. Rupp, "Enabling low-complexity MIMO in FBMCOQAM," in IEEE Globecom Workshops (GC Wkshps), Dec 2016.

[10] C. L´el´e, P. Siohan, R. Legouable, and M. Bellanger, "CDMA transmission with complex OFDM/OQAM," EURASIP Journal on Wireless Communications and Networking, vol. 2008, Article ID 748063, pp. 1– 12, 2008.

[11] R. Nissel, J. Blumenstein, and M. Rupp, "Block frequency spreading: A method for low-complexity MIMO in FBMC-OQAM," in IEEE Workshop on Signal Processing Advances in Wireless Communications (SPAWC), July 2017.

[12] A. Sahin, I. Guvenc, and H. Arslan, "A survey on multicarrier communications: Prototype filters, lattice structures, and implementation aspects," IEEE Communications Surveys Tutorials, vol. 16, no. 3, pp. 1312–1338, December 2012.

[13] Adoum, B. A., Zoukalne, K., Idriss, M. S., Ali, A. M., Moungache, A., & Khayal, M. Y. (2023). A Comprehensive Survey of Candidate Waveforms for 5G, beyond 5G and 6G Wireless Communication Systems. Open Journal of Applied Sciences, 13(01). https://doi.org/10.4236/ojapps.2023.131012.

[14] Alshami, S. (2021). Performance analysis of OFDMA, UFMC, and FBMC for optical wireless communication. 2021 1st International Conference on Emerging Smart Technologies and Applications, ESmarTA 2021. https://doi.org/10.1109/eSmarTA52612.2021.9515739

[15] A. Skrzypczak, J.-P. Javaudin, and P. Siohan, "Reduction of the peakto-average power ratio for the OFDM/OQAM modulation," in IEEE Vehicular Technology Conference, (VTC Spring), vol. 4, 2006, pp. 2018– 2022.

[16] C. Ye, Z. Li, T. Jiang, C. Ni, and Q. Qi, "PAPR reduction of OQAMOFDM signals using segmental PTS scheme with low complexity," IEEE Transactions on Broadcasting, vol. 60, no. 1, pp. 141–147, 2014.

[17] S. Sesia, M. Baker, and I. Toufik, LTE-the UMTS long term evolution: from theory to practice. John Wiley & Sons, 2011.

[18] D. Qu, S. Lu, and T. Jiang, "Multi-block joint optimization for the peak-to-average power ratio reduction of FBMC-OQAM signals," IEEE Transactions on Signal Processing, vol. 61, no. 7, pp. 1605–1613, 2013.

[19] T. Ihalainen, A. Viholainen, T. H. Stitz, M. Renfors, and M. Bellanger, “Filter bank based multi-mode multiple access scheme for wireless uplink,” in IEEE European Signal Processing Conference (EUSIPCO), 2009, pp. 1354–1358.

[20] C. H. Yuen, P. Amini, and B. Farhang-Boroujeny, “Single carrier frequency division multiple access (SC-FDMA) for filter bank multicarrier communication systems,” in IEEE International Conference on Cognitive Radio Oriented Wireless Networks (CROWNCOM), 2010, pp. 1–5.

[21] D. Na and K. Choi, “Low PAPR FBMC,” IEEE Transactions on Wireless Communications, vol. 17, no. 1, pp. 182–193, 2018

[22] T. Ihalainen, A. Viholainen, T. H. Stitz, M. Renfors, and M. Bellanger, “Filter bank based multi-mode multiple access scheme for wireless uplink,” in IEEE European Signal Processing Conference (EUSIPCO), 2009, pp. 1354–1358.